Highly Active Homogeneous Nickel Catalysts for Alkene Dimerisation: Crystal Structure of $[Ni(\eta^3\text{-}C_3H_5)(PPh_3)Br]$ and *in situ* Characterisation of $AlEt_3$-activated $[Ni(\eta^3\text{-}C_3H_5)(PPh_3)Br]$ by Nuclear Magnetic Resonance and Extended X-Ray Absorption Fine Structure Spectroscopy *

Paul Andrews, Judith M. Corker, John Evans and Michael Webster
Department of Chemistry, University of Southampton, Southampton SO9 5NH, UK

In situ NMR and extended X-ray absorption fine structure (EXAFS) spectroscopy have been used to characterise a highly active propene dimerisation catalyst, prepared by the low-temperature addition of $AlEt_3$ to $[Ni(\eta^3\text{-}C_3H_5)(PPh_3)Br]$. The molecular structure of $[Ni(\eta^3\text{-}C_3H_5)(PPh_3)Br]$ has been determined by X-ray crystallography and variable-temperature NMR spectroscopy. Crystal data: monoclinic, space group $P2_1/n$ (no. 14), $a = 7.951(1)$, $b = 14.954(1)$, $c = 16.096(3)$ Å, $\beta = 96.05(1)°$, $Z = 4$, $R = 0.045$. It has previously been assumed that aluminium interacts with nickel in such catalyst systems *via* halide-bridging ligands in order to decrease the charge on the nickel, thereby facilitating the co-ordination of electron donors to the nickel centre. EXAFS analysis provided direct structural evidence for a Ni···Al interaction in solution, but questioned the nature of the bridging ligand: the nickel K-edge EXAFS data of a solution of $[Ni(\eta^3\text{-}C_3H_5)(PPh_3)Br]$, $AlEt_3$ (Ni:Al = 1:5) and propene in toluene at −60 °C, showed that the first co-ordination sphere around nickel comprised 3.9 carbons at 1.93 Å and 1.0 phosphorus at 2.19 Å, with a more distant aluminium being present at 3.21 Å. Halide loss from the nickel centre is further confirmed by the bromine K-edge EXAFS data. These results implied Ni···Al interactions *via* alkyl bridges in the predominant solution species during catalysis. Phosphorus-31 NMR spectroscopy at −60 °C of the activated catalyst however showed at least four different species present. Halide loss from the nickel co-ordination sphere was also observed for the reaction of $AlBr_3$ with $[\{Ni(\eta^3\text{-}C_3H_5)Br\}_2]$ in toluene. The nickel K-edge EXAFS was best fitted by 9.0 carbons at 2.01 Å, providing strong evidence for the existence of $[Ni(\eta^3\text{-}C_3H_5)(\eta^6\text{-}C_6H_5Me)]^+\text{-}AlBr_4^-$.

The activation of nickel complexes by alkylaluminium cocatalysts is a well established method of producing homogeneous catalysts for the oligomerisation of alkenes into higher α-olefins.[1] These products have great industrial significance, being valuable intermediates in a variety of other processes (hydroformylation, copolymerisation, arylation, sulfonation) which lead, for example, to the production of plasticisers, solvents and surfactants.[2] Particular interest has focused on the application of allylnickel halide phosphine adducts $[Ni(\eta^3\text{-}C_3H_5)(PR_3)X]$ **1** (R = alkyl or aryl, X = Cl or Br) with alkylaluminium chloride cocatalysts towards propene dimerisation.[3–5] Turnovers of over 1 000 000 moles of propene per mole of nickel have been reported for such catalysts, making them some of the most active examples of homogeneous catalysts known.[5,6] Despite their extensive applications, the role of the aluminium reagents in such systems remains poorly defined. Other Lewis acids, such as BF_3 and $TiCl_4$, have been used successfully as activators[7] but the alkylaluminium halides appear to produce the best catalytic results over a wide range of systems. The reported isolation of the halide-bridged species **2** (X = Cl/Et) has prompted the assumption that the aluminium reagent will interact similarly with the nickel centre during catalysis.[5,8] Complete structural characterisation for complex **2** has, however, never been reported due to the high degree of disorder in the populations of the X groups and high thermal motion of the allyl group, which has prevented accurate structure refinement.

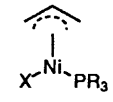

1

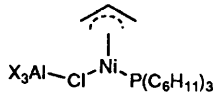

2

In a previous communication,[9] we showed how X-ray absorption, and in particular extended X-ray absorption fine structure (EXAFS) spectroscopy, could be used to probe the co-ordination sphere around nickel in order to provide direct structural information on the solution species present during the reaction of $Al_2Me_3Cl_3$ or $AlEt_3$ with $Ni(PEt_3)_2Cl_2$; a first co-ordination sphere consisting of only carbon and phosphorus was identified, showing that the halide ligands are removed from the nickel on reaction with the aluminium reagent. Additional Ni···Al shells at *ca.* 3 Å were also observed, implying Ni···Al interactions *via* alkyl bridges. It was suggested that these interactions are necessary to stabilise the organometallic centre, thus preventing decomposition to nickel metal. We have furthered our investigations into the role of aluminium in nickel oligomerisation catalysts and we now report detailed *in situ* nickel and bromine K-edge EXAFS studies on a low-temperature propene dimerisation catalyst derived from $[Ni(\eta^3\text{-}C_3H_5)(PPh_3)Br]$ and $AlEt_3$, with supporting evidence being provided by NMR spectroscopy. The reaction between $AlBr_3$ and $[\{Ni(\eta^3\text{-}C_3H_5)Br\}_2]$ in the absence of phosphine, for which loss of bromine from the nickel centre has been previously proposed,[10] is also discussed. X-Ray crystal structure and variable-temperature NMR data for

* *Supplementary data available:* see Instructions for Authors, *J. Chem. Soc., Dalton Trans.*, 1994, Issue 1, pp. xxiii–xxviii.

$[Ni(\eta^3\text{-}C_3H_5)(PPh_3)Br]$, obtained during the course of this work, are used to assist the interpretation of the *in situ* results.

One route to the synthesis of $[Ni(\eta^3\text{-}C_3H_5)(PPh_3)Br]$[11] is *via* the initial formation of $[\{Ni(\eta^3\text{-}C_3H_5)Br\}_2]$ **4**, by oxidative addition of the appropriate allyl halide to a nickel(0) complex such as $Ni(cod)_2$ **3** (cod = cycloocta-1,5-diene), the cyclooctadiene ligands being readily displaced. Treatment of the η^3-allylnickel halide **4** with PPh_3 then yields $[Ni(\eta^3\text{-}C_3H_5)(PPh_3)Br]$ **5**. Activation of **5** to afford the oligomerisation catalyst is then achieved by treatment with an excess of the alkylaluminium cocatalyst (Scheme 1). Allylnickel phosphine compounds generally have low thermal stabilities and are usually highly air sensitive, making them difficult to handle, and so a working system would require the initial generation of such a species *in situ* from less sensitive reagents, followed by activation within the cocatalyst. The direct characterisation of such a system under true reaction conditions, which should afford the most valuable information concerning the mode of operation of the catalyst, then often becomes too complicated since numerous reagents or species are present in solution at any one time. X-Ray absorption spectroscopy is, however, well suited to the *in situ* study of catalysts, but has had surprisingly little application in the field of homogeneous catalysis.[12]

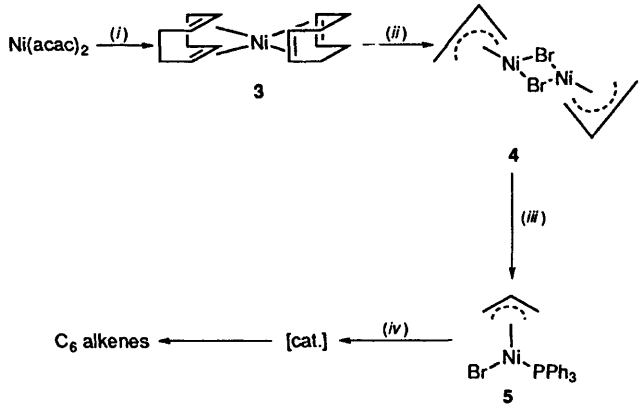

Scheme 1 (*i*) cod, $AlEt_3$, buta-1,3-diene in toluene at 10 °C; (*ii*) allyl bromide in toluene at −40 °C; (*iii*) PPh_3 in toluene at −40 °C; (*iv*) $AlEt_3$ in propene

We have used two approaches in order to characterise structurally by X-ray absorption spectroscopy the highly active $AlEt_3$-promoted $[Ni(\eta^3\text{-}C_3H_5)(PPh_3)Br]$–propene dimerisation catalyst. (*i*) Direct monitoring of the nickel centre during *in situ* generation and activation of $[Ni(\eta^3\text{-}C_3H_5)(PPh_3)Br]$ *via* the sequential addition of cycloocta-1,5-diene, allyl bromide, PPh_3 and $AlEt_3$ to $Ni(acac)_2$ (Hacac = acetylacetone) at low temperature; and (*ii*) validation of *in situ* results by separately examining the intermediate steps involved in catalyst generation and activation.

Results and Discussion

X-Ray Absorption Spectroscopic Studies during in situ *Generation of* $[Ni(\eta^3\text{-}C_3H_5)(PPh_3)Br]$ **5**.—Low-temperature, *in situ* EXAFS studies were carried out using a sampling system designed to allow the direct transfer of air-sensitive solutions into an aluminium cell attached to a Dewar vessel filled with the appropriate slush to maintain the desired temperature (Fig. 1). The desired solution, prepared in a reaction flask connected to a vacuum line, is flushed under argon through the X-ray absorption cell to an outlet flask, *via* stainless-steel needles. Gaseous reactants can also be introduced into the cell in a similar manner. Ice formation on the Kapton windows during cooling is prevented by enclosing the cell in a vacuum-tight box. Temperatures, monitored by a thermocouple connected to a digital thermometer, were found to vary within 5–10 °C of the desired value over a scan time of approximately 30 min. X-Ray absorption measurements can be made in both transmission and fluorescence data-collection modes with this cell.

Nickel K-edge EXAFS analysis (Fig. 2, Table 1) of a toluene solution containing $Ni(acac)_2$, cycloocta-1,5-diene, $AlEt_3$ and buta-1,3-diene (added to prevent nickel metal formation[14]) at 10 °C gave the expected first co-ordination sphere for $Ni(cod)_2$ of eight carbon atoms at 2.09 Å. An additional well defined shell of *ca.* eight carbons at 2.94 Å was also clearly identified. These

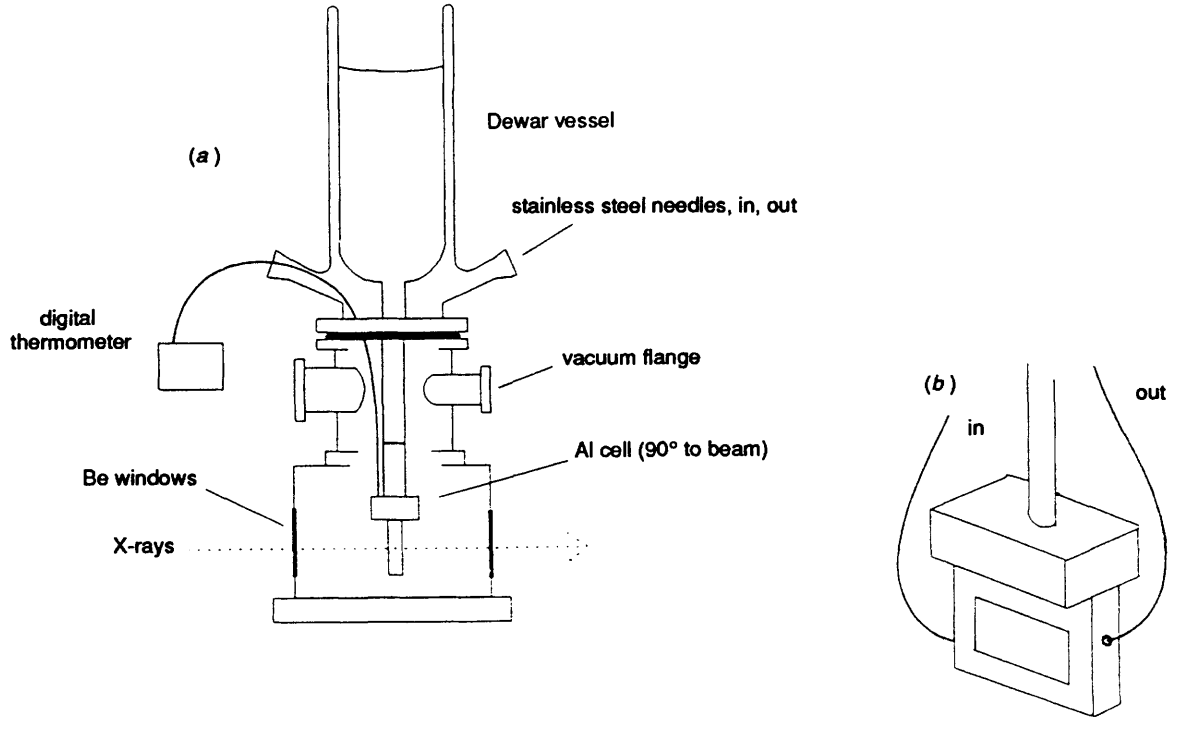

Fig. 1 Low-temperature X-ray absorption spectroscopy sampling system. (*a*) Cross-section of apparatus with cell at 90° to X-ray beam; (*b*) perspective view of the cell showing needles for sample introduction

EXAFS-derived distances are comparable to those obtained from the X-ray crystal structure of the solid[13] [average Ni–C and Ni · · · C distances are 2.122(8) and 2.98(4) Å respectively for the solid]. An almost identical EXAFS pattern was obtained for a pure, isolated sample of $Ni(cod)_2$ in toluene solution, with no significant differences in the EXAFS parameters being apparent. The above results suggest that the solid-state structure of $Ni(cod)_2$ is essentially maintained in solution. Having established that $Ni(cod)_2$ could be positively identified in a solution containing several other reagents, the subsequent reaction with allyl bromide was investigated. Addition of allyl bromide at −40 °C resulted in a dramatic change in the EXAFS pattern (Fig. 3, Table 1), the average co-ordination now being consistent with one allyl group (Ni–C 1.99 Å) and two bromine

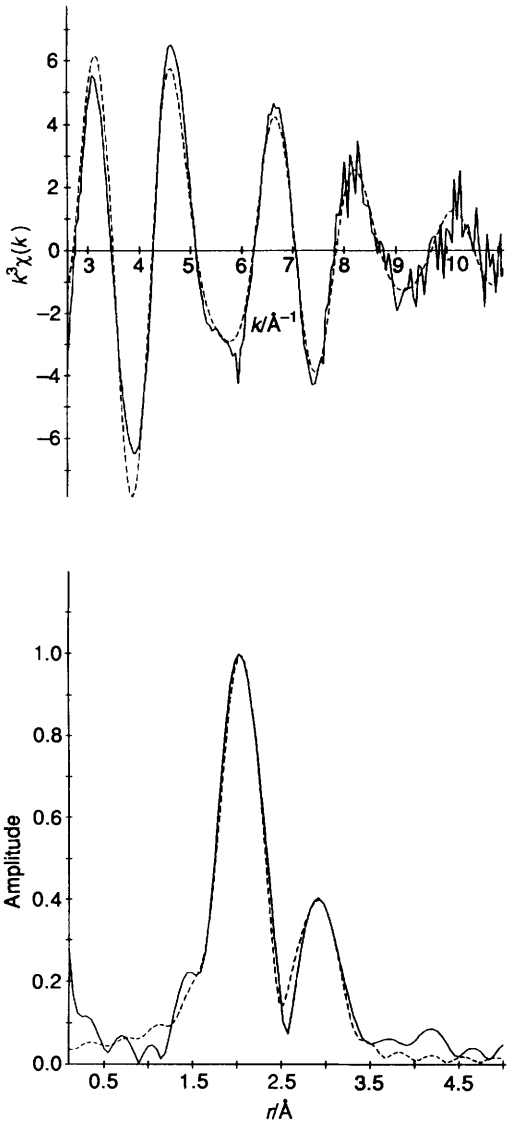

Fig. 2 The nickel K-edge k^3-weighted EXAFS data and Fourier transform, phase-shift corrected for carbon (———, experimental; – – – –, spherical wave theory), of $Ni(acac)_2$–cod–$AlEt_3$–buta-1,3-diene in toluene at 10 °C

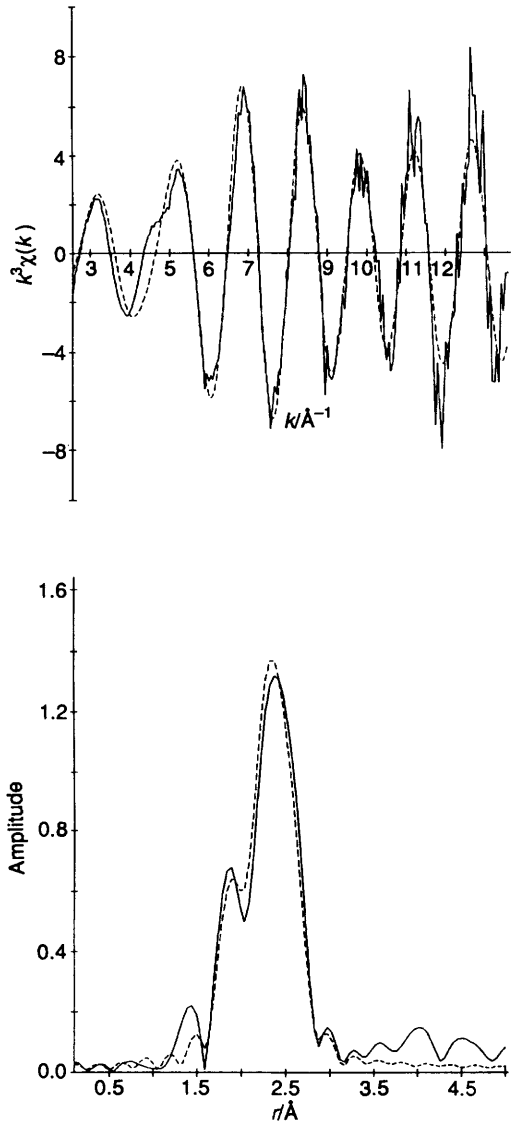

Fig. 3 The nickel K-edge k^3-weighted EXAFS data and Fourier transform, phase-shift corrected for carbon (——, experimental; – – – –, spherical wave theory), of $Ni(acac)_2$–cod–$AlEt_3$–buta-1,3-diene–allyl bromide in toluene at −40 °C

Table 1 Nickel K-edge EXAFS-derived structural parameters for various solutions in toluene

Solution	Shell	CN	r/Å	$2\sigma^2$[a]/Å^2	A_f[b]	E°/eV	E_v[c]/eV	R(%)
$Ni(acac)_2$–cod–$AlEt_3$–buta-1,3-diene	C	7.8	2.09[e]	0.018	0.8	22.1	−3.7	22.2
(10 °C)[d]	C	8.2	2.94[e]	0.025				
$Ni(acac)_2$–cod–$AlEt_3$–buta-1,3-diene–	C	2.9	1.99	0.006	0.8	15.2	−3.9	26.9
allyl bromide (−40 °C)[f]	Br	2.0	2.35	0.010				
$Ni(acac)_2$–cod–$AlEt_3$–buta-1,3-diene–PPh_3	C	3.1	2.03	0.010	0.8	14.2	−4.0	24.1
(−40 °C)[g]	P	0.9	2.21	0.005				
	Br	1.1	2.28	0.011				

[a] Debye–Waller factor; σ = root-mean-square internuclear separation. [b] Fraction of absorption causing EXAFS in 0.8 in all cases. [c] Virtual potential representing inelastic losses and core-hole lifetime effects. [d] [Ni] = 90 mmol dm^{-3}; Ni:Al:cod:C_4H_6 = 1:2:5: small excess. [e] Average X-ray data Ni–C and Ni · · · C distances for $Ni(cod)_2$ are 2.122(8) and 2.98(4) Å respectively.[13] [f] Ni:Br = 1:1. [g] Ni:P = 1:1.

atoms (Ni–Br 2.35 Å). No Ni ••• Ni distance is detectable in the Fourier transform which would have confirmed the presence of the expected dimeric species, $[\{Ni(\eta^3\text{-}C_3H_5)Br\}_2]$, in solution but the EXAFS-derived Ni–Br distance of 2.35 Å can be compared to the Ni–Br distance in $[\{Ni(\eta^3\text{-}C_3H_4CO_2Et)Br\}_2]$.[15] The absence of a Ni ••• Ni peak is surprising, but perhaps not totally unexpected: the presence of two heavy bromine back scatterers which dominate the EXAFS data, together with the large Debye–Waller factors associated with highly thermally populated low-frequency δ(Ni–Br–Ni) vibrations, presumably hinders observation of the more distant nickel. Separate experiments were carried out in order to isolate a pure sample of $[\{Ni(\eta^3\text{-}C_3H_5)Br\}_2]$, but decomposition generally resulted on attempting to recrystallise the crude product and thus was pursued no further.

A further change in the nickel K-edge EXAFS spectrum was again noted after the addition of PPh_3 to the $Ni(acac)_2$–cod–$AlEt_3$–buta-1,3-diene–allyl bromide solution at −40 °C. The EXAFS data were best fitted by a three-shell model of one phosphorus (2.21 Å), one bromine (2.28 Å) and three carbon atoms at 2.03 Å [Fig. 4(*a*), Table 1], suggesting the formation of $[Ni(\eta^3\text{-}C_3H_5)(PPh_3)Br]$ **5**. Attempts to model the EXAFS data using only two-shell models of either carbon and bromine or carbon and phosphorus resulted in unacceptable fits. The formation of a red solid was noted on removal of the solvent from this solution, from which dark red crystals of **5** could be isolated on recrystallisation.

The Structure of $[Ni(\eta^3\text{-}C_3H_5)(PPh_3)Br]$ **5**.—The crystal structure of complex **5** consists of discrete molecules (Fig. 5); selected bond lengths and angles are given in Table 2 and the atomic coordinates are listed in Table 3. The co-ordination geometry around nickel is as expected for a monomeric 16-electron η^3-allyl complex and the bond lengths are unexceptional. Related compounds include $[Ni(C_{10}H_{15})(PR_3)Br]$ ($C_{10}H_{15}$ = 2-pinen-10-yl),[16] $[Ni(\eta^3\text{-}C_3H_5)(PR_3)Cl]$[17] and $[Ni(\eta^3\text{-}C_3H_5)_2(PMe_3)]$.[18] The Ni–Br distance (2.315 Å) may be compared with the first compound (2.323 Å) and the Ni–P distance [2.196(2) Å] is a little shorter than the range of values from the above compounds (2.204–2.218 Å). Previous examples[16,17] involving phosphine and halide have been described in terms of a square-planar geometry at nickel with

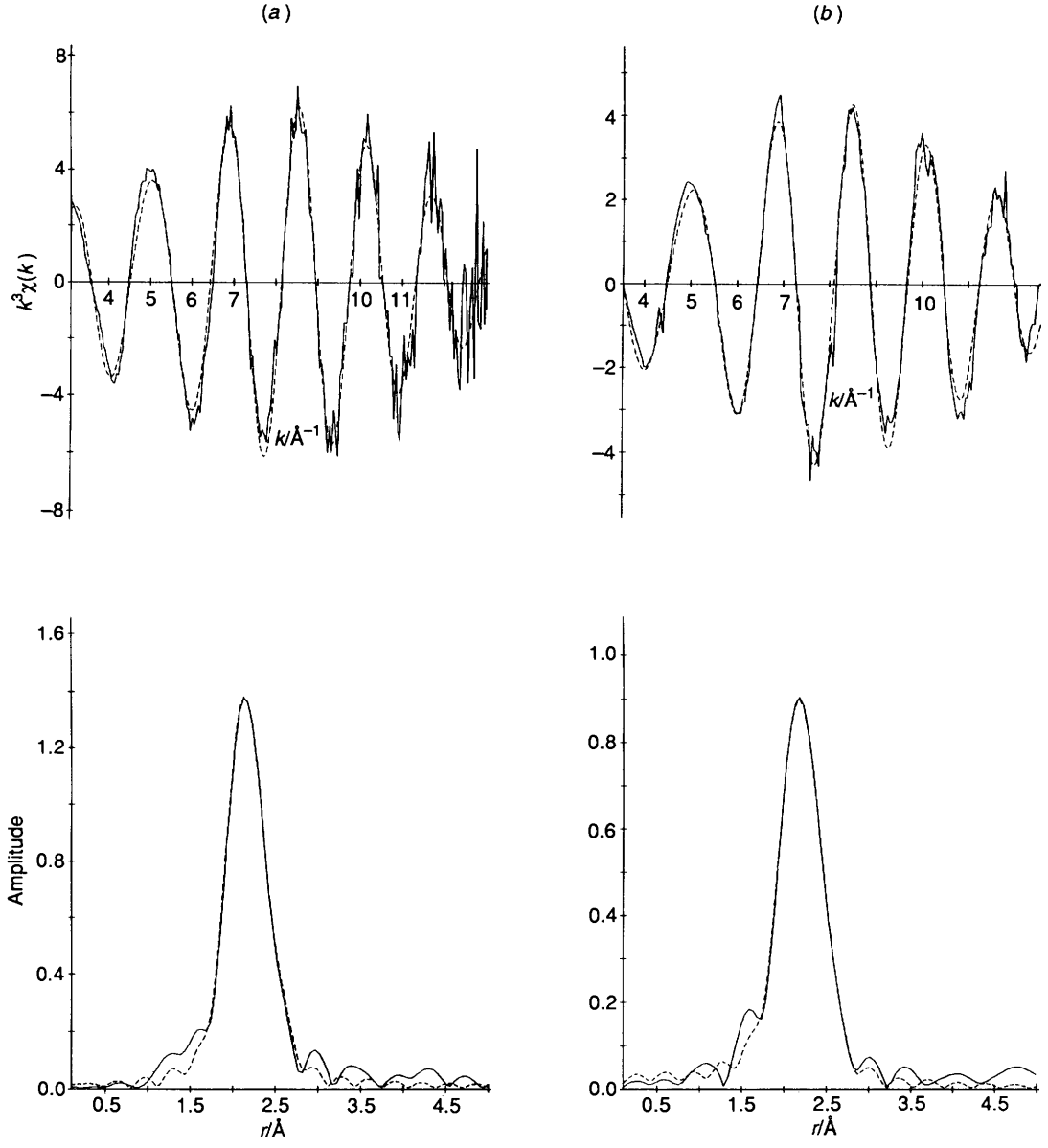

Fig. 4 The nickel K-edge k^3-weighted EXAFS data and Fourier transform, phase-shift corrected for carbon (—— experimental; – – – – spherical wave theory), of (*a*) $Ni(acac)_2$–cod–$AlEt_3$–buta-1,3-diene–allyl bromide–PPh_3 in toluene at −40 °C and (*b*) $[Ni(\eta^3\text{-}C_3H_5)(PPh_3)Br]$ (solid)

Table 2 Selected bond lengths (Å) and angles (°) for [Ni(η^3-C_3H_5)(PPh$_3$)Br]

Ni–Br	2.315(1)	Ni–P	2.196(2)
Ni–C(1)	2.07(1)	P–C(11)	1.843(9)
Ni–C(2)	1.95(1)	P–C(21)	1.842(8)
Ni–C(3)	2.03(1)	P–C(31)	1.825(8)
C(1)–C(2)	1.26(2)	C(2)–C(3)	1.40(2)
C–C (phenyl)	1.36(1)–1.41(1)		
P–Ni–Br	100.9(1)	C(1)–C(2)–C(3)	134.4(17)
C(1)–Ni–Br	91.4(4)	C(1)–Ni–P	165.4(4)
C(2)–Ni–Br	124.1(5)	C(2)–Ni–P	129.2(5)
C(3)–Ni–Br	164.7(3)	C(3)–Ni–P	94.1(3)
Ni–P–C(11)	119.1(3)	C(11)–P–C(21)	104.5(4)
Ni–P–C(21)	115.5(3)	C(11)–P–C(31)	103.0(4)
Ni–P–C(31)	109.7(3)	C(21)–P–C(31)	103.3(4)
P–C–C	117.7(7)–123.3(6)		
C–C–C (phenyl)	118.2(9)–121.7(9)		

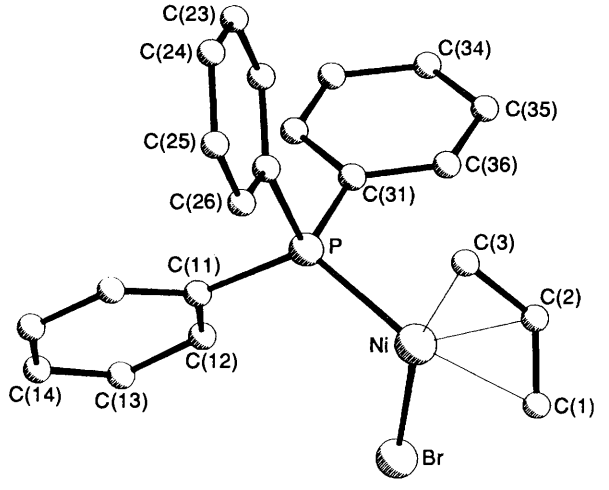

Fig. 5 Molecular structure of [Ni(η^3-C_3H_5)(PPh$_3$)Br] showing the atom numbering scheme. Phenyl H atoms omitted for clarity

the middle carbon atom of the C_3 residue out of the plane. On this description the maximum displacement from the plane of the five atoms in the co-ordination sphere is 0.07 Å and C(2) is 0.48 Å from the plane; the angle between this 'square-planar' best plane and the plane through the C_3 allyl residue is 116°.

Both nickel and bromine K-edge EXAFS data were also recorded for complex **5** at room temperature [Fig. 4(*b*)]. The Ni–P and Ni–Br interatomic distances of 2.19 and 2.30 Å respectively agree to within 0.01 Å of those obtained from the crystal structure, but the average Ni–C distance of 2.06 Å differs rather more significantly (0.04 Å) from the average X-ray value (Table 4). The EXAFS value does however lie within the range of X-ray Ni–C distances (1.95–2.07 Å). Analysis of the solution nickel and bromine K-edge EXAFS spectrum of isolated [Ni(η^3-C_3H_5)(PPh$_3$)Br] reveals comparable Ni–P and Ni–Br distances to those in the solid, but the average Ni–C distance (1.97 Å) again differs significantly from the value derived from the EXAFS of the solid. The discrepancy in Ni–C distances is most likely due to the allyl carbon distances falling into two categories, central (at 1.95 Å) and end carbons (2.03 and 2.07 Å, average 2.05 Å). A map of the EXAFS fit indices for the Ni–C distance *versus* the Ni–P distance for solid complex **5** does in fact illustrate this by showing an elongation of the minimum to higher interatomic distances in the Ni–C direction; the solid-state EXAFS fit has clearly adopted the slight dip in the fit-index minimum corresponding to the end carbons. The above results would seem to suggest that the structure of complex **5** does not alter significantly on dissolving in toluene.

Table 3 Atomic coordinates for [Ni(η^3-C_3H_5)(PPh$_3$)Br]

Atom	*x*	*y*	*z*
Ni	0.1451(1)	0.6169(1)	0.0076(1)
Br	0.1797(1)	0.5029(1)	−0.0864(1)
P	−0.0132(3)	0.7102(2)	−0.0718(1)
C(1)	0.3186(16)	0.5585(8)	0.0965(7)
C(2)	0.3026(23)	0.6416(11)	0.1065(9)
C(3)	0.1647(16)	0.6991(8)	0.1085(6)
C(11)	−0.1654(11)	0.6652(5)	−0.1557(5)
C(12)	−0.1022(11)	0.6235(6)	−0.2244(5)
C(13)	−0.2175(13)	0.5847(7)	−0.2851(6)
C(14)	−0.3885(13)	0.5900(7)	−0.2812(6)
C(15)	−0.4513(13)	0.6304(7)	−0.2150(7)
C(16)	−0.3405(12)	0.6682(7)	−0.1516(6)
C(21)	−0.1372(10)	0.7900(6)	−0.0159(5)
C(22)	−0.1383(11)	0.8812(6)	−0.0305(6)
C(23)	−0.2288(13)	0.9392(7)	0.0156(7)
C(24)	−0.3200(13)	0.9058(7)	0.0753(7)
C(25)	−0.3209(13)	0.8140(8)	0.0904(7)
C(26)	−0.2324(12)	0.7560(7)	0.0452(6)
C(31)	0.1207(10)	0.7825(5)	−0.1282(5)
C(32)	0.0609(11)	0.8272(6)	−0.2014(6)
C(33)	0.1656(13)	0.8826(7)	−0.2407(6)
C(34)	0.3318(13)	0.8937(6)	−0.2088(6)
C(35)	0.3904(11)	0.8511(7)	−0.1357(6)
C(36)	0.2854(11)	0.7954(6)	−0.0964(6)

X-Ray Absorption Spectroscopic Studies during Catalyst Activation with $AlEt_3$.—Treatment of the Ni(acac)$_2$–cod–allyl bromide–PPh$_3$ solution with propene at −40 °C appeared to cause no change in the nickel K-edge EXAFS pattern; disruption of the relatively stable allyl species by propene would anyway seem unlikely. Addition of excess $AlEt_3$ to this solution at −60 °C did however affect the X-ray absorption spectrum and a colour change from red to orange was noted. EXAFS analysis clearly shows that the bromine has been lost from the co-ordination sphere of the nickel. The best fit to the EXAFS data at this temperature was achieved with *ca.* four carbon atoms at 2.02 Å and one phosphorus at 2.20 Å [Fig. 6(*a*), Table 5], also suggesting that the allyl group is maintained. No change in the EXAFS pattern was observed on warming the solution to −10 °C. Aluminium co-ordination to nickel *via* bridging carbons was not conclusively detected in the EXAFS data of this sample; no significant peak around 3 Å was observed in the Fourier transform.

Parallel experiments involving the addition of propene and excess $AlEt_3$ to isolated complex **5** produced analogous nickel K-edge EXAFS results [Fig. 6(*b*)]. The first co-ordination sphere of the nickel is similarly best modelled by four carbons and one phosphine. No statistically valid bromine shell[19] could be fitted to the data, but some evidence does exist for the presence of a distant aluminium shell; a decrease in the *R* factor is observed when one aluminium is included at 3.21 Å but its validity must remain questionable due to the similarity in magnitude of other more distant peaks in the Fourier transform. Considering that $AlEt_3$ and similar aluminium alkyls have been used widely as alkylating agents in organonickel chemistry[1,20,21] and that complex **5** has been reported to react with alkylating agents such as methylmagnesium chloride to give alkylnickel species,[22] the increased carbon co-ordination suggests that complex **5** has been alkylated by $AlEt_3$. The alkyl group may be bridging between the nickel and the aluminium as in complex **6** (X = Br/Et), explaining the presence of an aluminium shell in the EXAFS when bromine is lost. Further confirmation for the loss of bromine from the first co-ordination sphere of the nickel following treatment with $AlEt_3$ is provided by the bromine K-edge EXAFS data [Fig. 7(*a*), Table 5]. These are best fitted by *ca.* two aluminiums at 2.47 Å and *ca.* two carbons at 3.59 Å, showing transfer of bromine from the nickel to the aluminium. When compared to the

Table 4 EXAFS-derived structural parameters for [Ni(η^3-C_3H_5)(PPh_3)Br]. Comparison with X-ray crystal structure interatomic distances

K-edge	Shell	CN	r/Å	$2\sigma^2$/Å^2	d(Ni–X)/Å	A_f	$E°$/eV	E_v/eV	R(%)
Solid									
Ni	C	3.0	2.06	0.020	1.95, 2.03, 2.07	0.80	13.7	−4.0	14.4
	P	1.0	2.19	0.014	2.20				
	Br	1.0	2.30	0.013	2.31				
Toluene solution									
Ni*	C	3.0	1.97	0.020		0.80	23.8	−4.0	18.9
	P	1.0	2.19	0.006					
	Br	1.0	2.30	0.006					
Br	Ni	1.0	2.30	0.007		0.81	11.4	−2.8	21.2

* [Ni] = 90 mmol dm^{-3}.

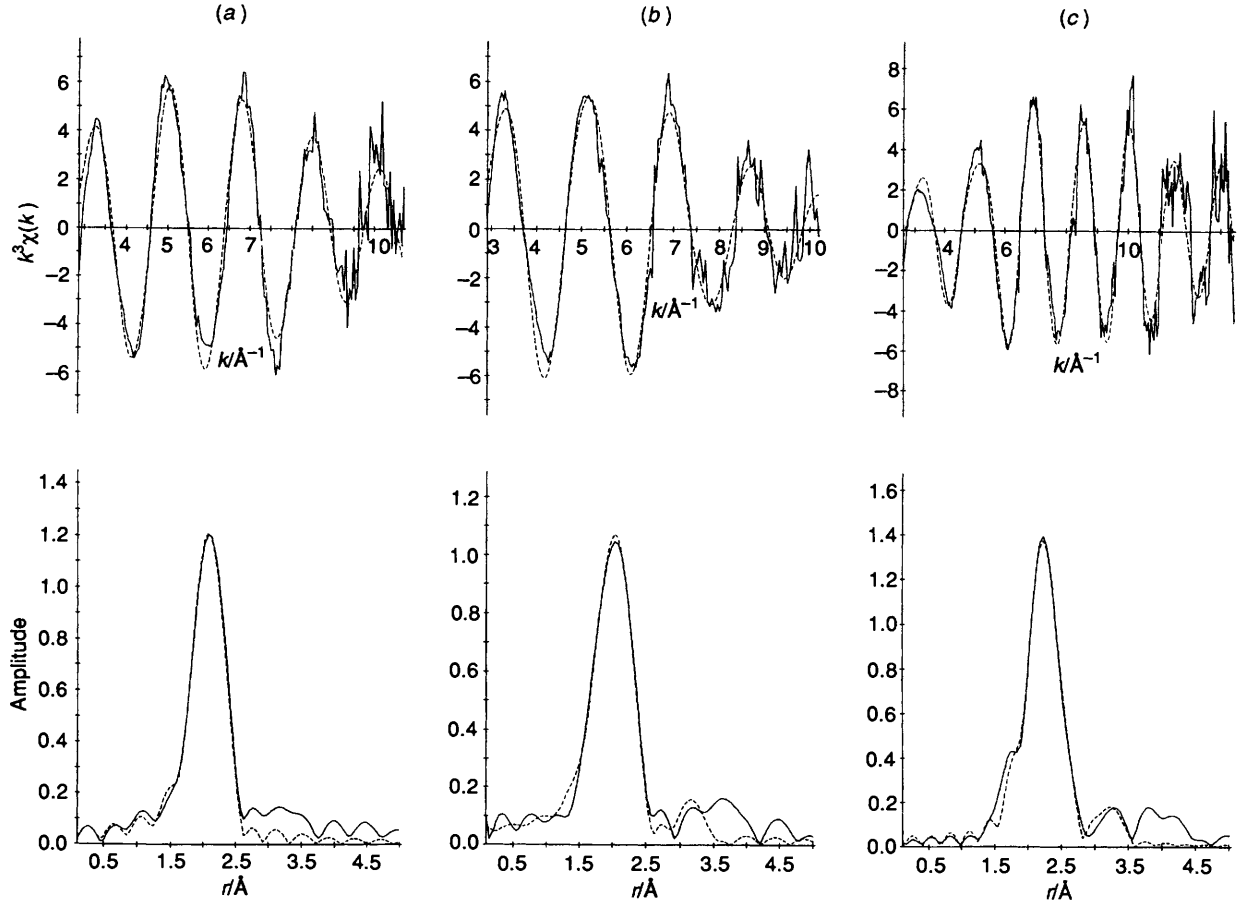

Fig. 6 The nickel K-edge k^3-weighted EXAFS data and Fourier transform, phase-shift corrected for carbon (——, experimental; – – –, spherical wave theory), of Ni(acac)$_2$–cod–allyl bromide–PPh_3–propene–$AlEt_3$ (*a*), [Ni(η^3-C_3H_5)(PPh_3)Br]–propene–$AlEt_3$ (Ni:Al = 1:5) (*b*) and [Ni(η^3-C_3H_5)(PPh_3)Br]–$AlEt_3$ (Ni:Al = 1:1) (*c*) in toluene at −60 °C

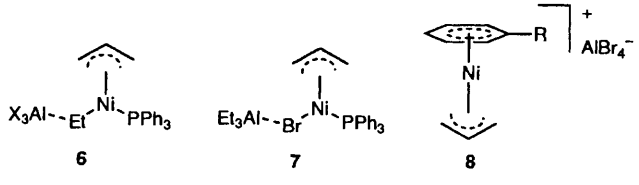

6 7 8

bridging or terminal distances in Al_2Br_6,* the EXAFS-derived Al–Br distance of 2.47 Å appears to be surprisingly long. To attempt to assess the validity of the bromine K-edge data for the [Ni(η^3-C_3H_5)(PPh_3)Br]–propene–$AlEt_3$ solution, solutions of aluminium bromide in toluene and allyl bromide in toluene were analysed separately. A good fit to the bromine K-edge EXAFS spectrum of aluminium bromide in toluene [Fig. 7(*b*), Table 5] was achieved using a four-shell model of aluminium (2.21 and 4.23 Å) and bromine (3.35 and 3.57 Å) atoms; these distances can be compared with those derived from the crystal-structure data for the solid* and are consistent with a dimeric structure in solution. A two-shell model of carbon atoms at 1.98 and 2.90 Å, was found to give the best fit to the bromine K-edge EXAFS data of allyl bromide

* Intramolecular distances for crystalline[23] (and gas phase[24]) Al_2Br_6: Br–Al 2.23 and 2.33 [2.21(4)], Br_b–Al 2.34 and 2.42 [2.33(4)], $Br_b \cdots Br_b$ 3.59 [3.20(10)], $Br_b \cdots Br_t$ 3.84 and 3.86 [3.78(10)] and $Br_t \cdots$ Al 4.75 and 4.78 [4.93(10)] Å.

Table 5 EXAFS-derived structural parameters for various solutions in toluene

Solution	K-edge	Shell	CN	r/Å	$2\sigma^2$/Å^2	A_f	$E°$/eV	E_v/eV	R(%)
$Ni(acac)_2$–cod–$AlEt_3$–allyl bromide–PPh_3–propene (−60 °C)[a]	Ni	C	3.8	2.02	0.014	0.90	20.0	−2.9	26.1
		P	1.3	2.20	0.007				
$[Ni(\eta^3\text{-}C_3H_5)(PPh_3)Br]$–$AlEt_3$–propene (−60 °C)[b]	Ni	C	3.9	1.93	0.018	0.80	19.2	−2.1	21.7
		P	1.0	2.19	0.005				
		Al	1.0	3.21	0.020				
	Br	Al	1.9	2.47	0.015	0.81	12.2	−2.6	29.0
		C	2.2	3.59	0.020				
$[Ni(\eta^3\text{-}C_3H_5)(PPh_3)Br]$–$AlEt_3$ (−60 °C)[c]	Ni	C	3.0	1.98	0.017	0.80	21.6	−4.0	28.7
		P	1.0	2.19	0.012				
		Br	1.0	2.31	0.006				
		Al	1.0	3.20	0.007				
	Br	Al	0.5	2.27	0.006	0.81	15.6	−2.3	36.0
		Al	1.3	2.51	0.005				
		C	1.5	3.47	0.015				
Aluminium bromide (25 °C)[d]	Br	Al	1.3	2.21	0.017	0.81	20.2	−2.2	19.4
		Br	0.3	3.35	0.009				
		Br	0.7	3.57	0.027				
		Al	1.0	4.23	0.014				
Allyl bromide (25 °C)[d]	Br	C	1.1	1.98	0.003	0.81	12.5	−2.5	20.7
		C	1.0	2.90	0.011				

[a] [Ni] = 90 mmol dm^{-3}; Ni:Al = 1:5. [b] [Ni] = 90 mmol dm^{-3}; Ni:Al = 1:5. [c] [Ni] = 90 mmol dm^{-3}; Ni:Al = 1:1. [d] [Br] = 90 mmol dm^{-3}.

in solution. Thus it was concluded that the aluminium and bromine central-atom phase shifts had been calculated sensibly and that the bromine K-edge EXAFS-derived structural parameters for the $[Ni(\eta^3\text{-}C_3H_5)(PPh_3)Br]$–propene–$AlEt_3$ solution were likely to be valid. However, the exact nature of the aluminium moiety is not clear; the EXAFS data point to the formation of a mixed alkyl bromide aluminium species, but little structural data are available for such complexes in solution to allow comparison.

The catalytic activity of $[Ni(\eta^3\text{-}C_3H_5)(PPh_3)Br]$–$AlEt_3$ towards the dimerisation of propene was monitored in a separate experiment under comparable conditions to the X-ray absorption spectroscopic experiments in order to confirm that an active catalyst solution was in fact being investigated during the EXAFS measurements. Gas-chromatographic analysis of a solution of $[Ni(\eta^3\text{-}C_3H_5)(PPh_3)Br]$ and $AlEt_3$ (Al:Ni 5:1) treated with propene for 1 h at −50 °C showed a 93% selectivity towards C_6 products and turnover of *ca.* 700 moles of propene per mole of nickel species.

More complicated behaviour was observed for 1:1 solutions of $AlEt_3$ and $[Ni(\eta^3\text{-}C_3H_5)(PPh_3)Br]$ which did not contain any propene. Little change from the nickel starting material was detected in the nickel K-edge EXAFS spectrum [Fig. 6(*c*), Table 5], but again, fits including a distant aluminium shell at *ca.* 3 Å were found to be acceptable, suggesting the formation of species **7**. Given the reported isolation of the halide-bridged complex **2**,[5,8] species **7** may reasonably exist in solution. The bromine K-edge EXAFS data were considerably different from that of the starting material, suggesting a substantial change in the chemical environment of the bromine. It appears that in the 1:1 case, the alkylation reaction has not gone to completion.

NMR Studies.—The ^{1}H NMR spectrum of complex **5** would be expected to contain five different signals due to the allyl ligand, but the observed resonances at room temperature (Table 6) are in fact consistent with an AM_2X_2 system. This is however a well documented phenomenon, arising from fluxionality within the molecule, and has been reported extensively for a variety of nickel, palladium and platinum allyl complexes.[1,11,25] Left-to-right exchange of *syn*- and *anti*-protons causes H^2 and H^3 to become equivalent, as well as H^4 and H^5. The signal for H^1 appears as a 'septet' but is in fact a triplet of triplets at δ 4.9, with the smaller *cis* coupling to H^2 and H^3 (7 Hz) being exactly half the magnitude of the *trans* coupling to H^4 and H^5 (14 Hz).

Table 6 NMR data for $[Ni(\eta^3\text{-}C_3H_5)(PPh_3)Br]$ and $[Ni(\eta^3\text{-}C_3H_5)(PPh_3)Br]$–$AlEt_3$ (200 mmol dm^{-3} Ni, Ni:Al = 1:5) in $[^2H_8]$toluene at various temperatures

Nucleus	T/°C	δ*
$[Ni(\eta^3\text{-}C_3H_5)(PPh_3)Br]$		
^{1}H	25	7.2–7.0 (m, 15 H, Ph), 4.9 (t of t, 1 H, H^1), 3.2 (d, 2 H, $^3J_{HH}$ 7, H^2 and H^3), 2.3 (d, 2 H, $^3J_{HH}$ 14, H^4 and H^5)
	−70	7.2–7.0 (m, 15 H, Ph), 4.8 (m, 1 H, H^1), 4.3 (s, 1 H, H^3), 3.1 (d of d, 1 H, $^3J_{HH}$ 13, $^3J_{HP}$ 5, H^5), 2.1 (s, 1 H, H^2), 1.5 (d, 1 H, $^3J_{HH}$ 13, H^4)
^{13}C-{^{1}H}	−70	134–130 (Ph), 110 (s, C^2), 74 (d, $^2J_{CP}$ 21, C^1), 57 (s, C^3)
^{31}P-{^{1}H}	25	−24 (s, PPh_3)
$[Ni(\eta^3\text{-}C_3H_5)(PPh_3)Br]$–$AlEt_3$		
^{31}P-{^{1}H}	−60	41, 33, 26, 22

* Coupling constants, J, in Hz.

The ^{1}H NMR spectrum at −70 °C however contains, as expected, five signals due to the allyl ligand, showing that exchange has been frozen. The average of the chemical shifts of the resonances for H^4 (δ 1.5) and H^5 (δ 3.1), and their couplings (13 Hz), confirms that they become equivalent at room temperature to give the signal at δ 2.3. Similarly, the average of the H^2 and H^3 shifts (δ 2.1 and δ 4.3) gives the resonance at δ 3.2 in the room-temperature spectrum. Their couplings could not however be resolved. The minor coupling on the resonance for H^5 (5 Hz) is due to phosphorus, indicating that H^5 is on the side of the allyl group *trans* to the phosphorus. Thus, the allyl protons *trans* to the phosphorus are downfield of those *trans* to bromine, so the resonances for H^3 and H^4 can be assigned. The ^{13}C NMR spectrum at −70 °C contains three resonances in the allyl region, consistent with the static structure. The exchange process could occur either *via* free rotation of the allyl group or through dissociation of the PPh_3 ligand; the latter mechanism is favoured here since P–H coupling is only observed at −70 °C and not at room temperature.

The ^{1}H NMR spectrum of $[Ni(\eta^3\text{-}C_3H_5)(PPh_3)Br]$ and $AlEt_3$ (1:5), recorded at −60 °C [Fig. 8(*a*)], is complex and firm conclusions are difficult to draw. The broad mass of signals between δ 0 and 1.7 are due to the aluminium reagent and contain no useful information. The signals from δ 2.0 to 6.0

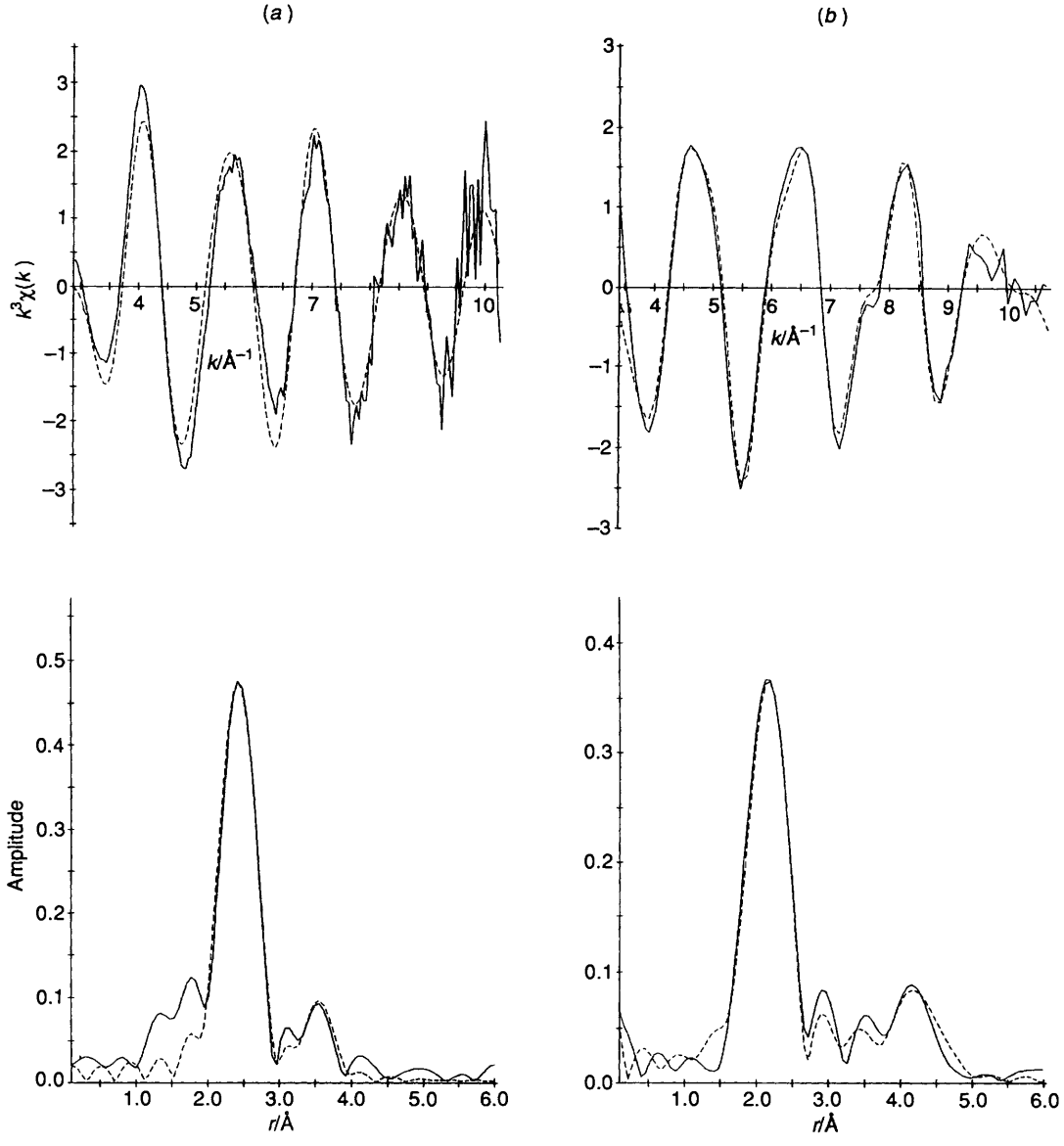

Fig. 7 The bromine K-edge k^3-weighted EXAFS data and Fourier transform, phase-shift corrected for aluminium (——, experimental; – – – –, spherical wave theory), of (*a*) [Ni(η^3-C_3H_5)(PPh_3)Br]–propene–$AlEt_3$ (Ni : Al = 1 : 5) in toluene at −60 °C, and (*b*) aluminium bromide in toluene at 25 °C

could be due to allyl groups. The resonances at δ 3.2 and δ 4.9 might be attributed to the starting material, but the absence of other signals would suggest that this species is no longer present. Carbon-13 NMR studies also afforded little information. Two conclusions could however be drawn from the ^{31}P NMR data at this temperature: at least four resonances are seen [Fig. 8(*b*), Table 6] that are not consistent with the starting material, and all of the phosphine remains co-ordinated to the nickel centre. These results illustrate the complex nature of these systems.

Reaction of [{Ni(η^3-C_3H_5)Br}$_2$] *with* $AlBr_3$.—Porri *et al.*[10] reported that the reaction of [{Ni(η^3-C_3H_5)Br}$_2$] with $AlBr_3$ in benzene led to the formation of ionic complexes of the type **8** (R = H) as oils which could be precipitated by the addition of *n*-heptane. The materials were characterised by elemental analysis and the presence of benzene in a 1 : 1 ratio with nickel was verified by chromatographic analysis, but no structural characterisation was reported. During our EXAFS investigation of the reaction between [{Ni(η^3-C_3H_5)Br}$_2$] [prepared *in situ* by the addition of allyl bromide to Ni(cod)$_2$] and $AlBr_3$ in toluene at −60 °C, the formation of a red-brown oil was similarly noted on addition of the aluminium reagent. The nickel K-edge EXAFS spectrum, although poor quality due to the limited solubility of the oil in the toluene solvent, clearly indicated that a single shell of *ca.* nine carbon atoms at an average distance of 2.01 Å is present around nickel. This provides strong evidence for the existence of **8** (R = Me), an 18-electron species.

Conclusion

Widespread discussion has taken place on the role of organoaluminium compounds in nickel-catalysed alkene oligomerisation. Proposed mechanisms are largely based on indirect evidence, *i.e.* the nature of products from catalytic reactions and the isolation of possible intermediates or related complexes.[1] It is generally assumed that the role of the Lewis acid is to decrease the charge on the nickel in order to facilitate the co-ordination of electron donors to the metal centre. This is proposed to occur *via* a halide bridge to aluminium (Fig. 9). Our EXAFS results do however strongly question this type of nickel–aluminium interaction: halide loss from the nickel co-ordination sphere is clearly evident in both the [Ni(η^3-C_3H_5)(PPh_3)Br]–$AlEt_3$–propene and [{Ni(η^3-C_3H_5)Br}$_2$]–$AlBr_3$ systems and combin-

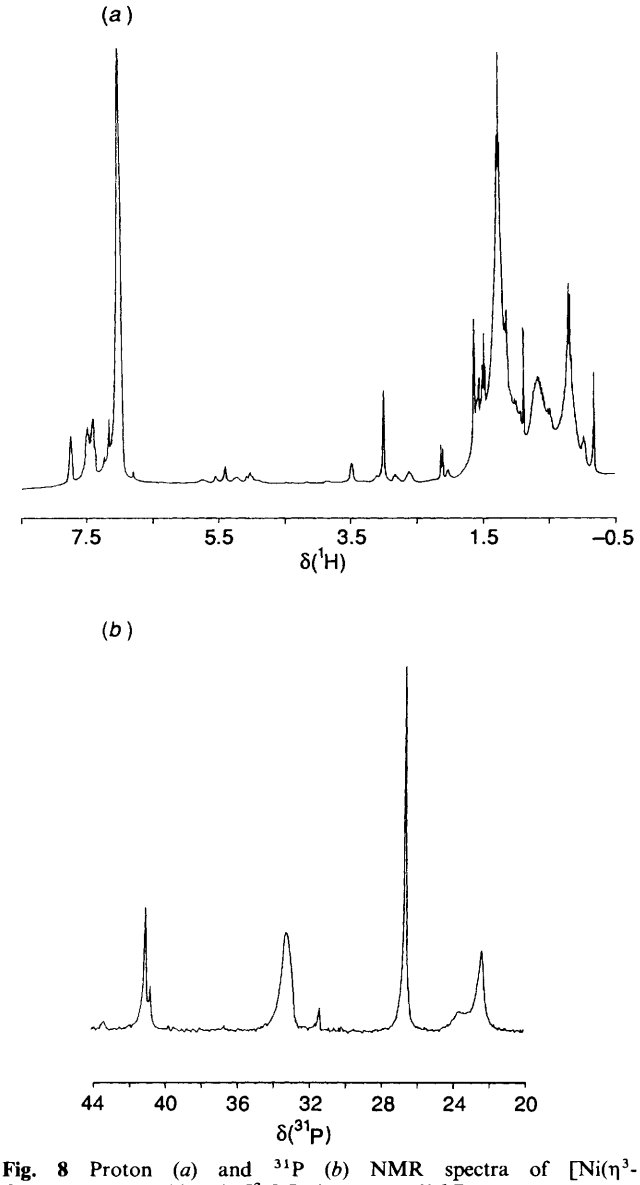

Fig. 8 Proton (*a*) and ^{31}P (*b*) NMR spectra of $[Ni(\eta^3\text{-}C_3H_5)(PPh_3)Br]$–$AlEt_3$ in $[^2H_8]$toluene at −60 °C

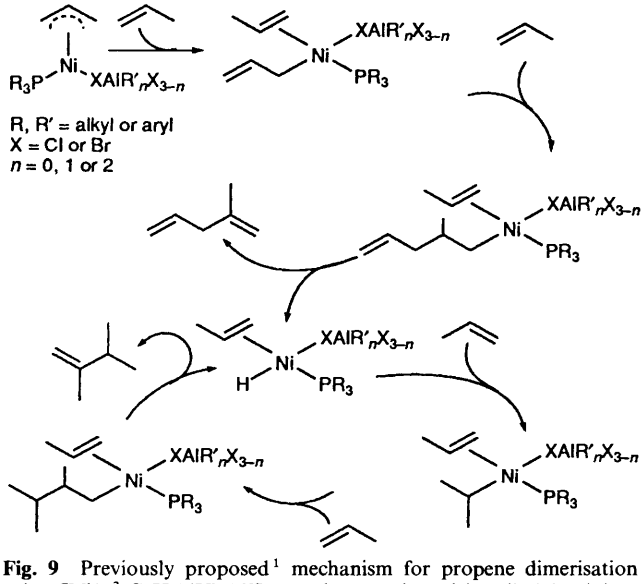

Fig. 9 Previously proposed[1] mechanism for propene dimerisation using $[Ni(\eta^3\text{-}C_3H_5)(PR_3)X]$ complexes activated by alkylaluminium halides

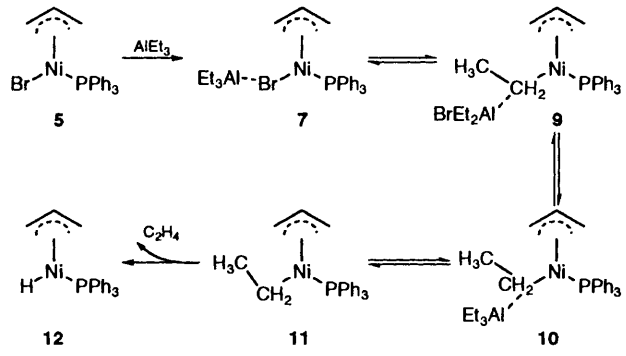

Fig. 10 Proposed activation reaction of $[Ni(\eta^3\text{-}C_3H_5)(PPh_3)Br]$ with $AlEt_3$, deduced from NMR and EXAFS spectroscopic studies. Species **12** has not been detected spectroscopically

ing the detection of a distant aluminium shell with the evidence of carbon and phosphorus co-ordination only around the nickel centre implies that an alkyl- rather than a halide-bridged species is present. Such reactions reflect how strong the drive is for the transfer of halide from the nickel centre to the Lewis acid. The exact nature of the most abundant species present during catalysis {*i.e.*, in the $[Ni(\eta^3\text{-}C_3H_5)(PPh_3)Br]$–$AlEt_3$–propene solution} is however still open to question. The first co-ordination sphere derived from the nickel K-edge EXAFS data could be interpreted in two ways. Either the allyl group is retained or it is replaced by a mixture of co-ordinated alkyl and alkene ligands, with the literature evidence and postulated mechanisms (Fig. 9) favouring the latter. Investigations on the fate of the allyl group during cyclooctene dimerisation using $[Ni(\eta^3\text{-}C_3H_5)(acac)]$–$Al_2Et_3Cl_3$ as the catalyst,[3] have demonstrated that *ca.* 80% of the allyl group originally bonded to nickel undergoes an initial reaction with cyclooctene, resulting in the formation of bicyclooctenes.

The EXAFS results also give direct structural evidence to support the retention of phosphine throughout the activation and catalysis process, which is entirely consistent with the fact that product selectivity is affected by the nature of the phosphine.[3–5] The ^{31}P NMR spectrum of $[Ni(\eta^3\text{-}C_3H_5)(PPh_3)Br]$–$AlEt_3$ in the absence of propene, however, reveals that a number of species are present in the activated solution. The NMR data could be accommodated by the presence of complex **7**, some alkyl-bridged species **9** and **10**, and the non-bridged product of alkylation complex **11**. The alkylation of the nickel centre could be envisaged as a route to the formation of a catalytically active hydride **12** *via* β-hydrogen transfer and elimination of ethene from complex **11** (Fig. 10). It should however be noted that ethylaluminium reagents do not apparently afford catalysts which are significantly more active than their methylaluminium analogues, which cannot undergo β-hydride elimination after alkylation of the nickel centre. This suggests that this route is not the major pathway to hydride formation. It does seem likely though that the reported halide-bridged species **2** is only one of several intermediates present during the activation process, with the halide bridge being lost before the formation of the active species. The technique of X-ray absorption spectroscopy has thus proved extremely valuable in providing direct structural information on a highly complex, active homogeneous catalyst system.

Experimental

All manipulations were carried out under a nitrogen or argon atmosphere, using standard Schlenk techniques. All solvents were dried and distilled under nitrogen prior to use. Buta-1,3-diene (98%) and $AlEt_3$ (93%) were obtained from Aldrich and used without further purification. Cycloocta-1,5-diene was distilled prior to use. The reagents $Ni(cod)_2$[14] and anhydrous

$Ni(acac)_2$ [26] were prepared using methods previously described. Gas chromatography was carried out on a Perkin-Elmer Autosystem gas chromatograph, using a BP1 (dimethylsiloxane stationary phase) capillary column. Samples for the NMR studies were prepared in a dry nitrogen glove box fitted with a liquid nitrogen-cooled metal block to allow low-temperature manipulation of reagents. Proton, ^{13}C and ^{31}P NMR spectra were recorded using a Bruker AM 360 spectrometer, with the ^1H and ^{13}C chemical shifts reported relative to $SiMe_4$ and the ^{31}P chemical shifts relative to 85% H_3PO_4. Samples for the X-ray absorption spectroscopic studies were prepared *in situ* by sequential addition of reagents and then transferred *via* cannula into the X-ray absorption cell.

Synthesis of [$Ni(\eta^3\text{-}C_3H_5)(PPh_3)Br$] **5**.—Allyl bromide (0.35 cm^3, 4.0 mmol) was added dropwise to a stirred suspension of $Ni(cod)_2$ (0.67 g, 4.0 mmol) in toluene (10 cm^3) at −78 °C. Triphenylphosphine (1.05 g, 4.0 mmol) in toluene (5 cm^3) was then introduced and the solution warmed to room temperature, during which time the $Ni(cod)_2$ dissolved and the yellow solution turned dark red. The solvent was removed under vacuum to leave a solid red residue. Impurities were removed by dissolving the crude product in hot toluene (80 °C) and filtering. The dark red crystals of **5**, formed on cooling the filtrate, were isolated, washed with cold toluene and dried under vacuum. Yield = 1.66 g (56%). NMR data are given in Table 6.

EXAFS Data Acquisition and Analysis.—X-Ray absorption spectra were recorded on stations 7.1 [Si(111) order-sorting monochromator] and 9.2 [Si(220) order-sorting monochromator] of the Synchrotron Radiation Source at the Daresbury Laboratory, operating at 2 GeV (*ca.* 3.20 × 10^{-10} J) and an average current of 150 mA. Data were acquired either in transmission mode, or in fluorescence mode using a single Tl–NaI scintillation counter fitted with a Co filter. Background-subtracted EXAFS data were obtained using the program PAXAS.[27] Removal of the pre-edge background was achieved using a polynomial of order 2. For the nickel K-edge spectra, the post-edge background was subtracted by fitting this region with a polynomial of order 6 or 7. The bromine K-edge spectra however, required coupled polynomials (order 7 or 8) to be fitted to the post-edge region to eliminate low frequency contributions in the spectra. Curve-fitting analyses, by least-squares refinement of the non-Fourier filtered k^3-weighted EXAFS data were carried out within EXCURVE,[28] using spherical-wave methods with *ab initio* phase shifts and back-scattering factors calculated in the usual manner from relativistic HF–SCF derived atomic-charge densities. Model compounds with known co-ordination sphere bond lengths were used to establish the transferability of phase-shift parameters.[29] No modification of calculated phase shifts was found to be necessary. Precision on Ni···X and Br···X distances is considered to be 1.4 and 1.6% for bonded and non-bonded distances respectively[29] and precision on co-ordination numbers are *ca.* 0.5. The statistical validity of shells was assessed by published means[19] and the numbers of independent parameters used in the fits are within the guideline, $N_{pts} = 2(k_{max} - k_{min})(R_{max} - R_{min})/\pi$ (ref. 30). The R factors are defined as $(\int|\chi^T - \chi^E|k^3dk/\int|\chi^E|k^3dk) \times 100\%$.

Crystal Structure Determination of [$Ni(\eta^3\text{-}C_3H_5)(PPh_3)Br$].—Air-sensitive, dark red crystals of the compound were obtained from toluene solution and sealed in thin-wall glass capillaries. Preliminary X-ray photographic examination established the crystal system and approximate cell dimensions. The density was measured by flotation.

Crystal data. $C_{21}H_{20}BrNiP$, M = 441.96, monoclinic, space group $P2_1/n$ (no. 14), a = 7.951(1), b = 14.954(1), c = 16.096(3) Å, β = 96.05(1)°, U = 1903.1 Å^3, Z = 4, D_c = 1.542, D_m = 1.52(2) g cm^{-3}, λ(Mo-Kα) = 0.710 69 Å, μ(Mo-Kα) = 31.4 cm^{-1}, F(000) = 896, ambient temperature.

Data collection. Data were collected on an Enraf-Nonius FAST area-detector diffractometer equipped with Mo-Kα radiation and graphite monochromator. Cell dimensions were obtained from 250 reflections and intensity data for 9349 reflections were recorded (approximate hemisphere of data, θ_{max} 29.8°). Lorentz-polarisation corrections were applied during the data processing.[31] Systematic absences established the space group, and after averaging there remained 4670 unique reflections (R_{int} = 0.088). No absorption correction was applied.

Structure solution and refinement. The position of the bromine, nickel and phosphorus atoms emerged from the application of SHELXS 86[32] and repeated structure-factor and electron-density calculations located all the carbon atoms. The later difference electron-density maps showed clear evidence for the phenyl H atoms and these were introduced into the model in fixed positions. The allyl H atoms were not convincingly located. Full-matrix least-squares refinement[33] converged to R = 0.045 {1708 reflections [$F > 3\sigma(F)$], 217 parameters, anisotropic (Ni, Br, P, C) and isotropic (H) atoms, $w^{-1} = [\sigma^2(F) + 0.001F^2]$, maximum shift/error = 0.09, R' = 0.059}. The residual electron density was in the range 0.54 to −0.54 e Å^{-3}. Neutral-atom scattering factors and anomalous-dispersion corrections were taken from SHELX 76[33] and ref. 34 (Ni) and the calculations were carried out using SHELX 76,[33] SHELXS 86[32] and PLUTO[35] on an IBM 3090 computer.

Additional material available from the Cambridge Crystallographic Data Centre comprises H-atom coordinates, thermal parameters and remaining bond lengths and angles.

Acknowledgements

We thank the SERC (J. M. C. and P. A.) and BP Research (J. M. C.) for support, the Director of the Daresbury Laboratory for the provision of facilities, and Professor M. B. Hursthouse and the SERC for the X-ray data collection.

References

1 P. W. Jolly and G. Wilke, *The Organic Chemistry of Nickel*, Academic Press, New York, 1974, vol. 1; 1975, vol. 2.
2 W. Keim, *Angew. Chem., Int. Ed. Engl.*, 1990, **29**, 235.
3 B. Bogdanovic, *Adv. Organomet. Chem.*, 1979, **17**, 105.
4 B. Bogdanovic, B. Henc, H.-G. Karmann, H.-G. Nussel, D. Walter and G. Wilke, *Ind. Eng. Chem.*, 1970, **62**, 34.
5 G. Wilke, *Angew. Chem., Int. Ed. Engl.*, 1988, **27**, 206.
6 B. Bogdanovic, B. Splietoff and G. Wilke, *Angew. Chem., Int. Ed. Engl.*, 1980, **19**, 622.
7 S. G. Abasowa, *Neftekhimiya*, 1973, **13**, 46; N. V. Petrushanskaya, A. I. Kurapova, N. M. Rodionova and V. Sh. Feldblyum, *Zh. Org. Khim.*, 1974, **10**, 1402; K. Maruya, T. Mizoroki and A. Ozaki, *Bull. Chem. Soc. Jpn.*, 1973, **46**, 993.
8 B. Bogdanovic, B. Henc, A. Losler, B. Meister, H. Pauling and G. Wilke, *Angew. Chem., Int. Ed. Engl.*, 1973, **12**, 954.
9 J. M. Corker and J. Evans, *J. Chem. Soc., Chem. Commun.*, 1991, 1104.
10 L. Porri, G. Natta and M. C. Gallazi, *J. Polym. Sci., Part C*, 1967, **6**, 2525.
11 E. Carmona, P. Palma and M. L. Poveda, *Polyhedron*, 1990, **9**, 757.
12 B. R. Stults, R. M. Friedman, K. Koenig, W. Knowles, R. B. Greegor and F. Lytle, *J. Am. Chem. Soc.*, 1981, **103**, 3235; J. Goulon, E. Georges, C. Goulon-Ginet, Y. Chauvin, D. Commereuc, H. Dexpert and E. Freund, *Chem. Phys.*, 1984, **83**, 357.
13 H. Dierks and H. Dietrich, *Z. Kristallogr., Kristallgeom., Kristallphys., Kristallchem.*, 1965, **122**, 1.
14 R. A. Schunn, *Inorg. Synth.*, 1974, **15**, 5.
15 M. R. Churchill and T. A. O'Brian, *Inorg. Chem.*, 1967, **6**, 1386.
16 C. Kruger, *Chem. Ber.*, 1976, **109**, 3574.
17 H. Brandes, R. Goddard, P. W. Jolly, C. Kruger, R. Mynott and G. Wilke, *Z. Naturforsch., Teil B*, 1984, **39**, 1139.
18 B. Henc, P. W. Jolly, R. Salz, S. Stobbe, G. Wilke, R. Benn, R. Mynott, K. Seevogel, R. Goddard and C. Kruger, *J. Organomet. Chem.*, 1980, **191**, 449.
19 R. W. Joyner, K. J. Martin and P. Meehan, *J. Phys. C.*, 1987, **20**, 4005.
20 T. Yamamoto, M. Takamatsu and A. Yamamoto, *Bull. Chem. Soc. Jpn.*, 1982, **55**, 325.

21 F. A. Cotton, B. A. Benz and D. L. Hunter, *J. Am. Chem. Soc.*, 1974, **96**, 4820.
22 B. Bogdanovic, H. Bonneman and G. Wilke, *Angew. Chem., Int. Ed. Engl.*, 1966, **5**, 582.
23 P. A. Renes and C. H. MacGillavry, *Recl. Trav. Chim. Pays-Bas*, 1945, **64**, 275.
24 K. J. Palmer and N. Elliot, *J. Am. Chem. Soc.*, 1938, **60**, 1852.
25 P. W. Jolly, *Comprehensive Organometallic Chemistry*, eds. G. Wilkinson, F. G. A. Stone and E. Abel, Pergamon, Oxford, 1982, vol. 6, p. 145; J. K. Becconsall, B. E. Job and S. O'Brian, *J. Chem. Soc. A*, 1967, 423; G. Wilke, *J. Organomet. Chem.*, 1980, **191**, 425, 449.
26 R. G. Charles and M. A. Pawlikowski, *J. Phys. Chem.*, 1958, **62**, 440.
27 N. Binsted, PAXAS Program for the analysis of X-ray absorption spectra, University of Southampton, 1988.
28 S. J. Gurman, N. Binsted and I. Ross, *J. Phys. C*, 1984, **17**, 143; 1986, **19**, 1845.
29 J. M. Corker, J. Evans, H. Leach and W. Levason, *J. Chem. Soc., Chem. Commun.*, 1988, 181.
30 F. W. Lytle, D. E. Sayers and E. A. Stern, *Physica B + C (Amsterdam)*, 1989, **158**, 701.
31 M. B. Hursthouse, A. I. Karaulov, M. Ciechanowicz-Rutkowska, A. Kolasa and W. Zankowska-Jasinska, *Acta Crystallogr., Sect. C*, 1992, **48**, 1257; P. A. Bates, S. A. Islam and M. J. E. Sternberg, *Acta Crystallogr., Sect. C*, 1993, **49**, 300.
32 G. M. Sheldrick, SHELXS 86, Program for solution of crystal structures, University of Göttingen, 1986.
33 G. M. Sheldrick, SHELX 76, Program for crystal structure determination, University of Cambridge, 1976.
34 *International Tables for X-Ray Crystallography*, Kynoch Press, Birmingham, 1974, vol. 4, pp. 99, 149.
35 W. D. S. Motherwell and W. Clegg, PLUTO, Program for plotting molecular and crystal structures, Universities of Cambridge and Göttingen, 1978.

Received 7th September 1993; *Paper* 3/05343A